


A regularization method based on level-sets for the problem of crack detection from electrical measurements

A De Cezaro¹ , E Hafemann², A Leitão^{2,*}  and A Osses³

¹ Institute of Mathematics, Statistics and Physics, Federal University of Rio Grande, Rio Grande, Brazil

² Department of Mathematics, Federal University of St. Catarina, PO Box 476, 88040-900 Florianópolis, Brazil

³ DIM/CMM, Universidad de Chile, Beauchef 851, Edificio Norte, piso 5, Casilla 170/3 Correo 3, Santiago, Chile

E-mail: acgleitao@gmail.com

Received 19 June 2022; revised 6 December 2022

Accepted for publication 27 January 2023

Published 15 February 2023



CrossMark

Abstract

We investigate regularization methods for solving the problem of crack detection in bounded planar domains from electrical measurements on the boundary. Based on the multiple level-set approach introduced in Álvarez *et al* (2009 *J. Comput. Phys.* **228** 5710–21) and on the regularization strategy devised in De Cezaro *et al* (2009 *Inverse Problems* **25** 035004), we propose a Tikhonov type method for stabilizing the inverse problem. Convergence and stability results for this Tikhonov method are proven. An iterative method of (multiple) level-set type is derived from the optimality conditions for the Tikhonov functional, and a relation between this method and the iterated Tikhonov method is established. The proposed level-set method is tested on the same benchmark problem considered in Álvarez *et al* (2009 *J. Comput. Phys.* **228** 5710–21). The numerical experiments demonstrate its ability to identify cracks in different scenarios with high accuracy even in the presence of noise.

Keywords: crack detection, electrical measurements, level-set methods, Tikhonov regularization

(Some figures may appear in colour only in the online journal)

* Author to whom any correspondence should be addressed.

1. Introduction

The presence of cracks drastically reduces the structural strength of materials. Hence, the development of methods for crack detection from indirect measurements becomes a paramount issue. This inverse problem is related to non-destructive testing and finds application in techniques used in the science and technology industry, e.g. [3, 8, 16, 20, 21, 25, 33] and references therein. In contrast to elastic materials [8, 32], crack identification in the electromagnetic medium is considered in the setting of inverse scattering (see, e.g. [12, 34]) or in impedance imaging with boundary measurement (see, e.g. [3, 8, 16, 22, 29]). Crack reconstruction approaches includes shape optimization methods [3, 12, 23, 24, 34], reciprocity principle [32], probe method [22], factorization method [6, 7, 19], asymptotic analysis [9], among others.

In this manuscript, we investigate the problem of determine both position and shape of a crack in a material represented as bounded domain $\Omega \subset \mathbb{R}^2$, from a finite set on N electrical measurements on the boundary $\partial\Omega$ related to the Neumann-to-Dirichlet map [26, 27].

As a model problem, we assume that the domain Ω has Lipschitz boundary and represents the specimen under investigation, in which a set of currents profiles $\{\eta_j\}_{j=1}^N$ are applied at the boundary $\partial\Omega$, for with, we have access to measurements of the corresponding potentials $\{u_j\}_{j=1}^N$ only on $\partial\Omega$ (i.e. we measure $u_j|_{\partial\Omega}$). Furthermore, we investigate problems constituted by an insulating crack with finite conductivity $b(x)$, that represent a high contrast between the interior and the exterior of the crack⁴. In other words, we assume that a crack can be modeled as a thin structure with small thickness $\beta > 0$ along a curve contained in Ω , satisfying the system of Neumann boundary values problem (BVP)

$$\nabla \cdot (b(x)\nabla u_j(x)) = 0, \quad x \in \Omega, \quad b(x)(u_j(x))_\nu = \eta_j(x), \quad x \in \partial\Omega, \quad (1)$$

with $\int_{\partial\Omega} \eta_j = 0$, for $j = 1, \dots, N$ (here $(u_j(x))_\nu$ denotes the normal derivative of u_j at $x \in \partial\Omega$).

We further adopt the following parameter space for the conductivity b given by $D_F := \{b \in L^\infty(\Omega); \bar{b} \geq b(x) \geq \underline{b} > 0, \text{ a.e. in } \Omega\} \subset X := \{b \in L^\infty(\Omega); b(x) \geq \underline{b} > 0, \text{ a.e. in } \Omega\}$. Assuming that the boundary data $\eta_j \in H^{-1/2}(\partial\Omega)$ in (1), then, it is well known that the system of Neumann BVP (1) has a unique solution $u_j \in H_*^1 := \{u \in H^1(\Omega); \int_{\partial\Omega} u_j = 0\}$, for each $j = 1, \dots, N$, e.g. [14].

Therefore, the crack detection problem can be written in terms of the system of nonlinear operator equations

$$\begin{aligned} F_j : D_F \subset X &\rightarrow Y \\ b &\mapsto F_j(b) = u_j|_{\partial\Omega} =: \gamma_j \end{aligned} \quad (2)$$

where $Y := H^{1/2}(\partial\Omega)$ and $u_j|_{\partial\Omega}$ is the Dirichlet trace (e.g. [1]) of the corresponding solution u_j for the BVP (1), for each $j = 1, \dots, N$. Hence, the crack problem under investigation is related to the electrical impedance tomography problem for the Neumann-to-Dirichlet (NtD) operator with a finite number N of measurements [5, 26, 27].

In practical applications the exact data $\gamma_j \in Y$, for $j = 1, \dots, N$ is, in general, not known. Instead, one disposes only an approximate measured data $\gamma_j^\delta \in Y$ satisfying

$$\sum_{j=1}^N \|\gamma_j^\delta - \gamma_j\|_Y \leq \delta, \quad (3)$$

⁴ See section 2 for a precise representation of b .

where $\delta > 0$ is the noise level.

Our formulation and numerical computation concerns cracks with a small and fixed thickness of size $\beta > 0$ and known conductivity and background conductivity values (see the details in section 2). The main results in this article can be summarized as follows:

- (a) We prove that any forward map F_j in (2), for $j = 1, \dots, N$ is continuous in the $L^1(\Omega)$ -topology (see proposition 4). Such property is necessary to establish regularization properties for the level set approximated solutions for the inverse problems.
- (b) The position and shape of the crack are parameterized by a pair of level set functions (see section 2). A Tikhonov functional based on a TV- H^1 penalization is proposed and analyzed (see section 3). We prove that this generates a regularization method for the crack identification problem in (2) and (3).
- (c) The optimality conditions for the Tikhonov functional allow the derivation of a stable level-set type method (namely, an iterated-Tikhonov type method) for the crack identification problem.

This article is outlined as follows: In section 2, we formulate the level set modeling setting for the crack detection. In section 3, we prove regularization properties of the level set approach for the crack detection. In section 4, we formulate the numerical approach and derives the algorithm used in the numerical experiments presented in section 5. Section 6, is devoted to some final remarks and conclusions.

2. Modeling the parameter space

In order to model the space of admissible parameters (cracks), we use the approach proposed in [3]. According to this representation strategy a level set function $\varphi : \Omega \rightarrow \mathbb{R}$ is chosen in such a way that its zero level-set $\Gamma_\varphi := \{x \in \Omega; \varphi(x) = 0\}$ defines a connected curve within Ω and that the cracks are located ‘along’ Γ_φ . Moreover, a second level-set function $\psi : \Omega \rightarrow \mathbb{R}$ is chosen such that the intersections of the level-set curve $\Gamma_\psi := \{x \in \Omega; \psi(x) = 0\}$ with Γ_φ coincide with the endpoints of the cracks, and the cracks are contained in $\{x \in \Omega; \psi(x) > 0\}$. Therefore, the position of the cracks corresponds to the set

$$S = S(\varphi, \psi) := \Gamma_\varphi \cap \{x \in \Omega; \psi(x) > 0\}.$$

In the ‘ideal insulating crack’ case (with zero thickness $\beta = 0$), the set S correspond to a proper subset of Γ_φ and the strategy above allow us to exactly represent the cracks (in a non unique way), see [3].

In this article, we assume the cracks have fixed thickness $\beta > 0$ (and $\beta \ll 1$) and conductivity $b_i > 0$ much smaller than the background value $b_e > 0$, where all the three constants β, b_i, b_e are known. Therefore, the position of the cracks can be represented by the set

$$S_\beta = S_\beta(\varphi, \psi) := \Gamma_\varphi^\beta \cap \{x \in \Omega; \psi(x) > 0\},$$

where $\Gamma_\varphi^\beta := \{x \in \Omega; -\beta/2 < \varphi(x) < \beta/2\}$.

Consequently, the conductivity distribution in (1) can be modeled by

$$b(x) = b_e + (b_i - b_e)\chi_{S_\beta}(x), \quad (4)$$

where χ_{S_β} is the indicator function of the set S_β .

It is worth noticing that in (4) a multiple level-set representation (see, e.g. [10] and references therein) of the unknown parameter b is proposed. Following [10], we introduce the Heaviside projector

$$(H(\varphi))(x) := \begin{cases} 1, & \text{if } \varphi(x) > 0 \\ 0, & \text{if } \varphi(x) \leq 0 \end{cases},$$

define the ‘symmetric translation’ $(H_\beta(\varphi))(x) := H(\varphi(x) + \beta/2) - H(\varphi(x) - \beta/2)$, and write the conductivity distribution $b(x)$ in the form

$$b = (b_i - b_e)H_\beta(\varphi)H(\psi) + b_e =: P(\varphi, \psi). \quad (5)$$

As already observed in [10], the operator H maps $H^1(\Omega)$ into the space

$$\mathcal{V}_{0,1} := \{w \in L^\infty(\Omega) \mid w = \chi_S, S \subset \Omega \text{ measurable}, \mathcal{H}^1(\partial S) < \infty\}, \quad (6)$$

where $\mathcal{H}^1(S)$ denotes the one-dimensional Hausdorff measure of the set S . Thus, the operator P in (5) maps $H^1(\Omega) \times H^1(\Omega)$ into the admissible class $\mathcal{V} \subset X$ defined by

$$\mathcal{V} := \{w \in L^\infty(\Omega) \mid w = b_e + (b_i - b_e)\chi_S, S \subset \Omega \text{ measurable}, \mathcal{H}^1(\partial S) < \infty\}. \quad (7)$$

In the forthcoming analysis, we write $P(\varphi, \psi) := q(H(\varphi + \beta/2), H(\varphi - \beta/2), H(\psi))$, where the operator $q : (L^\infty(\Omega))^3 \rightarrow L^\infty(\Omega)$ is defined as

$$q : (z^1, z^2, z^3) \mapsto (b_i - b_e)(z^1 - z^2)z^3 + b_e. \quad (8)$$

Within this framework, the inverse problem (2) with data given as in (3) can be written in the form of the system of operator equations

$$F_j(P(\varphi, \psi)) = \gamma_j^\delta, j = 1, \dots, N. \quad (9)$$

Once an approximate solution (φ, ψ) of (9) is calculated, a corresponding approximate solution of (2) is obtained in a straightforward way, indeed, $b = P(\varphi, \psi)$.

3. Tikhonov regularization

Here, we follow [10] and introduce the Tikhonov functional

$$\begin{aligned} \mathcal{G}_\alpha(\varphi, \psi) := & \sum_{j=1}^N \|F_j(P(\varphi, \psi)) - \gamma_j^\delta\|_Y^2 + \alpha \left(\mu_1 |H(\varphi + \beta/2)|_{\text{BV}} + \mu_2 |H(\varphi - \beta/2)|_{\text{BV}} \right. \\ & \left. + \mu_3 |H(\psi)|_{\text{BV}} + \mu_4 \|\varphi - \varphi_0\|_{H^1(\Omega)}^2 + \mu_5 \|\psi - \psi_0\|_{H^1(\Omega)}^2 \right) \end{aligned} \quad (10)$$

based on TV- H^1 penalization, where $\alpha > 0$ plays the role of a regularization parameter. The H^1 -terms act simultaneously as a control on the size of the norm and as a regularization on the space $H^1(\Omega)$ (here $\varphi_0, \psi_0 \in H^1(\Omega)$ are reference level-set functions). The BV-seminorm terms are well known for penalizing the length of the Hausdorff measure of the boundary of the sets $\{x : \varphi(x) > -\beta/2\}$, $\{x : \varphi(x) < \beta/2\}$ and $\{x : \psi(x) > 0\}$ (see [15]). The constants μ_j for $j \in \{1, \dots, 5\}$ are weight parameters.

3.1. Choosing the parameter space

Once the Tikhonov functional has been chosen, we concentrate on the task of finding an adequate parameter space to minimize $\mathcal{G}_\alpha(\varphi, \psi)$ in (10). We start posing some general assumptions to the model.

- (A1) $\Omega \subseteq \mathbb{R}^2$ is bounded with piecewise C^1 boundary $\partial\Omega$.
- (A2) System (9) has a solution, i.e. there exists $b^* \in \mathcal{U}$ satisfying $F_j(b^*) = \gamma_j, j = 1, \dots, N$. Moreover, there exist functions $\varphi^*, \psi^* \in H^1(\Omega)$ satisfying $P(\varphi^*, \psi^*) = b^*$, with $|\nabla \varphi^*| \neq 0, |\nabla \psi^*| \neq 0$ in a neighborhood of $\{\varphi^* \in [-\beta/2, \beta/2]\}, \{\psi^* = 0\}$ respectively. We further assume that $H(\varphi^* + \beta/2) = z^1, H(\varphi^* - \beta/2) = z^2, H(\psi^*) = z^3$, for some $z^1, z^2, z^3 \in \mathcal{V}_{0,1}$.

The choice of the parameter space (as well as its topology) should be such that existence of minimizers for the functional \mathcal{G}_α in (10) can be guaranteed. This is not the case as explained in the following remark.

Remark 1. According to the model exposed in section 2, the unknown parameter b is to be modeled by $b = P(\varphi, \psi) = q(\mathcal{O}(\varphi, \psi))$, where

$$\mathcal{O} : (H^1(\Omega))^2 \ni (\varphi, \psi) \longmapsto [H(\varphi - \beta/2), H(\varphi + \beta/2), H(\psi)] \in (L^\infty(\Omega))^3.$$

However, since H is discontinuous, the graph of the operator \mathcal{O} is not closed as a subset of $(L^\infty(\Omega))^3 \times (H^1(\Omega))^2$. Consequently, it is not possible to guarantee that minimizing sequences for the functional \mathcal{G}_α have limit in $(L^\infty(\Omega))^3 \times (H^1(\Omega))^2$.

With the remark 1 in mind, we adapt the concept of generalized minimizers introduced in [10] to the framework described above. As we shall see in definition 1 below, we introduce an extended parameter space (the so-called set of admissible quintuples), which corresponds to the closure of the graph of \mathcal{O} in $(L^\infty(\Omega))^3 \times (H^1(\Omega))^2$ with respect to a topology related to the concept of Γ -convergence [4]. Furthermore, we redefine the Tikhonov functional $\mathcal{G}_\alpha(\varphi, \psi)$ on this extended parameter space in order to introduce a new concept of (generalized) minimizers of \mathcal{G}_α .

Before introducing the generalized minimizers, we define the operators $\{H_\varepsilon\}_{\varepsilon>0}$

$$H_\varepsilon(\varphi) := \begin{cases} 0, & \text{if } \varphi < -\varepsilon \\ 1 + \varphi/\varepsilon, & \text{if } \varphi \in [-\varepsilon, 0] \\ 1, & \text{if } \varphi > 0 \end{cases},$$

which represent continuous approximations to the operator H . Analogously, we define the approximations $\{P_\varepsilon\}_{\varepsilon>0}$ to the operator P by

$$P_\varepsilon(\varphi, \psi) := (b_i - b_e)H_{\beta,\varepsilon}(\varphi)H_\varepsilon(\psi) + b_e, \quad (11)$$

where $H_{\beta,\varepsilon}(\varphi) := H_\varepsilon(\varphi + \frac{\beta}{2}) - H_\varepsilon(\varphi - \frac{\beta}{2})$.

Definition 1. Let the operators $H_\varepsilon, H_{\beta,\varepsilon}$ be defined as above.

- (a) A quintuple of functions $(z^1, z^2, z^3, \varphi, \psi) \in (L^\infty(\Omega))^3 \times (H^1(\Omega))^2$ is called **admissible** if there exist sequences $\{\varphi_k, \psi_k\}_{k \in \mathbb{N}}$ in $(H^1(\Omega))^2$, and a sequence of positive numbers $\varepsilon_k \rightarrow 0$ such that

$$\lim_{k \rightarrow \infty} \|\varphi_k - \varphi\|_{L^2(\Omega)} = 0, \quad \lim_{k \rightarrow \infty} \|\psi_k - \psi\|_{L^2(\Omega)} = 0,$$

$$\begin{aligned} \lim_{k \rightarrow \infty} \|H_{\varepsilon_k}(\varphi_k + \frac{\beta}{2}) - z^1\|_{L^1(\Omega)} &= \lim_{k \rightarrow \infty} \|H_{\varepsilon_k}(\varphi_k - \frac{\beta}{2}) - z^2\|_{L^1(\Omega)} \\ &= \lim_{k \rightarrow \infty} \|H_{\varepsilon_k}(\psi_k) - z^3\|_{L^1(\Omega)} = 0. \end{aligned}$$

- (b) A minimizer of $\hat{\mathcal{G}}_\alpha$ is considered to be any admissible quintuple of the form $(z^1, z^2, z^3, \varphi, \psi)$ minimizing

$$\hat{\mathcal{G}}_\alpha(z^1, z^2, z^3, \varphi, \psi) := \|F(q(z^1, z^2, z^3)) - y^\delta\|_Y^2 + \alpha \rho(z^1, z^2, z^3, \varphi, \psi) \quad (12)$$

over all admissible quintuples. Here the functional ρ is defined by

$$\begin{aligned} \rho(z^1, z^2, z^3, \varphi, \psi) := \inf \left\{ \liminf_{k \rightarrow \infty} \left(\mu_1 |H_{\varepsilon_k}(\varphi_k + \frac{\beta}{2})|_{\text{BV}} + \mu_2 |H_{\varepsilon_k}(\varphi_k - \frac{\beta}{2})|_{\text{BV}} \right. \right. \\ \left. \left. + \mu_3 |H_{\varepsilon_k}(\psi_k)|_{\text{BV}} + \mu_4 \|\varphi_k - \varphi_0\|_{H^1}^2 + \mu_5 \|\psi_k - \psi_0\|_{H^1}^2 \right) \right\}, \quad (13) \end{aligned}$$

where the infimum is taken with respect to all sequences $\{\varepsilon_k\}_{k \in \mathbb{N}}$ and $\{\varphi_k, \psi_k\}_{k \in \mathbb{N}}$ satisfying (a).

- (c) A **generalized minimizer** of $\mathcal{G}_\alpha(\varphi, \psi)$ is a minimizer of $\hat{\mathcal{G}}_\alpha(z^1, z^2, z^3, \varphi, \psi)$ on the set of admissible quintuples.

In what follows, we present some remarks related to definition 1.

Remark 2. The set of admissible quintuples is to be considered as a topological space, namely a subset of $(L^\infty(\Omega))^3 \times (H^1(\Omega))^2$ endowed with the topology of $(L^1(\Omega))^3 \times (L^2(\Omega))^2$. The closedness of this extended parameter space, which contains the generalized minimizers of \mathcal{G}_α is analyzed in lemma 2.

Remark 3. Let $\varphi^*, \psi^* \in H^1(\Omega)$ satisfying Assumption (A2). Define the constant sequence $\{(\varphi_k, \psi_k) = (\varphi^*, \psi^*)\}_{k \in \mathbb{N}}$. Then, arguing with the co-area formula [15, chapter 4], we can prove that

$$\|H_{\varepsilon_k}(\varphi_k + \beta/2) - z^1\|_{L^1} \rightarrow 0, \|H_{\varepsilon_k}(\varphi_k - \beta/2) - z^2\|_{L^1} \rightarrow 0, \|H_{\varepsilon_k}(\psi_k) - z^3\|_{L^1} \rightarrow 0$$

as $k \rightarrow \infty$ (see [10, remark 1] for details). Now, from definition 1, we conclude that $(z^1, z^2, z^3, \varphi^*, \psi^*)$ is an admissible quintuple. Consequently, it follows from assumption (A2) that the set of admissible quintuples satisfying $F_j(P(\varphi, \psi)) = \gamma_j$ is not empty.

Remark 4. From definition 1 (b), it follows that for each admissible quintuple $(z^1, z^2, z^3, \varphi, \psi) \in (L^\infty(\Omega))^3 \times (H^1(\Omega))^2$ the functional ρ in (13) is the Γ -limit of the sequence of functionals $\rho_k(\varphi, \psi) := \mu_1 |H_{\varepsilon_k}(\varphi + \frac{\beta}{2})|_{\text{BV}} + \mu_2 |H_{\varepsilon_k}(\varphi - \frac{\beta}{2})|_{\text{BV}} + \mu_3 |H_{\varepsilon_k}(\psi)|_{\text{BV}} + \mu_4 \|\varphi - \varphi_0\|_{H^1}^2 + \mu_5 \|\psi - \psi_0\|_{H^1}^2$, where $\{\varepsilon_k\}_{k \in \mathbb{N}}$ is a sequence on which the infimum on the right hand side of (13) is attained.

Moreover, from the fact that ρ is a Γ -limit together with the Γ -convergence definition [4, section 6], we conclude that ρ is lower semi-continuous on the set of admissible quintuples w.r.t. the topology described in remark 2.

Next, we verify some basic properties of the operators P_{ε_k} , H_{ε_k} and q that are necessary in the forthcoming analysis

Lemma 1. Under assumption (A1) the following assertions hold true:

- Let $\{(z_k^1, z_k^2, z_k^3)\}_{k \in \mathbb{N}} \in (\mathcal{V}_{0,1})^3$ be a sequence converging in $(L^1(\Omega))^3$ to some element $(z^1, z^2, z^3) \in (\mathcal{V}_{0,1})^3$. Then $q(z_k^1, z_k^2, z_k^3) \rightarrow q(z^1, z^2, z^3)$ in $L^1(\Omega)$.
- Let $(z^i, \varphi, \psi) \in L^\infty(\Omega)^3 \times H^1(\Omega)^2$ be such that $H_\varepsilon(\varphi + \beta/2) \rightarrow z^1$, $H_\varepsilon(\varphi - \beta/2) \rightarrow z^2$, $H_\varepsilon(\psi) \rightarrow z^3$ in $L^1(\Omega)$ as $\varepsilon \rightarrow 0$. Then $P_\varepsilon(\varphi, \psi) \rightarrow q(z^1, z^2, z^3)$ in $L^1(\Omega)$ as $\varepsilon \rightarrow 0$.
- Given $\varepsilon > 0$, let $\{(\varphi_k, \psi_k)\}_{k \in \mathbb{N}}$ be a sequence in $(H^1(\Omega))^2$ converging to $(\varphi, \psi) \in (H^1(\Omega))^2$ in the L^2 -norm. Then $H_\varepsilon(\varphi_k + \beta/2) \rightarrow H_\varepsilon(\varphi + \beta/2)$, $H_\varepsilon(\varphi_k - \beta/2) \rightarrow H_\varepsilon(\varphi - \beta/2)$ and $H_\varepsilon(\psi_k) \rightarrow H_\varepsilon(\psi)$ in $L^1(\Omega)$, as $k \rightarrow \infty$.

Proof. Assertion (a) follows from the estimate

$$\begin{aligned} \|q(z_k^1, z_k^2, z_k^3) - q(z^1, z^2, z^3)\|_{L^1} &\leq \int_{\Omega} |b_i - b_e| |(z_k^1 - z^1)z_k^3 - (z^1 - z^2)z^3 \pm (z^1 - z^2)z_k^3| \\ &\leq |b_i - b_e| \int_{\Omega} (|z_k^1 - z^1| + |z_k^2 - z^2|) |z_k^3| + |z^1 - z^2| |z_k^3 - z^3| \\ &\leq 2|b_i - b_e| \int_{\Omega} (|z_k^1 - z^1| + |z_k^2 - z^2| + |z_k^3 - z^3|), \end{aligned}$$

where in the last inequality we used the fact $z^i, z_k^i \in \mathcal{V}_{0,1}$. The proof of assertion (b) follows a similar argument. For a proof of assertion (c) we refer the reader to [10, lemma 1]. \square

The following result guarantees the closedness of the set of admissible quintuples with respect to the $(L^1(\Omega))^3 \times (L^2(\Omega))^2$ convergence (see definition 1). The prove follow the lines of the proof of [10, lemma 2].

Lemma 2. *Let $\{(z_k^1, z_k^2, z_k^3, \varphi_k, \psi_k)\}_{k \in \mathbb{N}}$ be a sequence of admissible quintuples converging in $(L^1(\Omega))^3 \times (L^2(\Omega))^2$ to some $(z^1, z^2, z^3, \varphi, \psi) \in (L^\infty(\Omega))^3 \times (H^1(\Omega))^2$. Then $(z^1, z^2, z^3, \varphi, \psi)$ is an admissible quintuple.*

In the next lemma, we verify the coerciveness and lower semi-continuity of the functional ρ on the set of admissible quintuples.

Lemma 3. *For each admissible quintuple $(z^1, z^2, z^3, \varphi, \psi)$, we have*

$$\sum_{i=1}^3 \mu_i |z^i|_{BV} + \mu_4 \|\varphi - \varphi_0\|_{H^1}^2 + \mu_5 \|\psi - \psi_0\|_{H^1}^2 \leq \rho(z^1, z^2, z^3, \varphi, \psi). \quad (14)$$

Moreover, given a sequence $\{(z_k^1, z_k^2, z_k^3, \varphi_k, \psi_k)\}_{k \in \mathbb{N}}$ of admissible quintuples such that $z_k^i \rightarrow z^i$ in $L^1(\Omega)$, $\varphi_k \rightharpoonup \varphi$ in $H^1(\Omega)$, $\psi_k \rightharpoonup \psi$ in $H^1(\Omega)$, where $(z^1, z^2, z^3, \varphi, \psi)$ is some admissible quintuple, then ρ is weak-lower semi-continuous, i.e. satisfies

$$\rho(z^1, z^2, z^3, \varphi, \psi) \leq \liminf_{k \in \mathbb{N}} \rho(z_k^1, z_k^2, z_k^3, \varphi_k, \psi_k).$$

Proof. What concerns the lower semi-continuity property of ρ , this issue is addressed in remark 4. The proof of the coercivity property in (14) follows the lines of the proof in [10, lemma 4]. \square

3.2. Convergence analysis

As we have seen in lemmas 1 and 2, the set of generalized admissible parameters shall be considered endowed with the $L^1(\Omega)$ -topology. Therefore, for the convergence analysis of the Tikhonov approach, we shall be able to prove the continuity of forward operators F_j in (2) w.r.t. the $L^1(\Omega)$ -topology. It is the content of the following proposition (for L^p continuity results of the forward operator in the Complete Electrode Model, see [28]).

Proposition 4. *Let the boundary data in the BVP (1) satisfy $\eta_j \in (W^{1-1/q, q}(\partial\Omega))'$, for $q = p/(p-1)$, for any $p \in]2, p_0[$, where $p_0 > 2$ is an adequate constant. Then, the operators $F_j : D(F) \subset L^1(\Omega) \rightarrow Y$ are continuous on $D(F)$ with respect to the $L^1(\Omega)$ -topology.*

Although proposition 4 is quintessential for the forthcoming convergence analysis (theorems 5–7), a proof is postponed to section 3.3. In what follows, we prove that for any regularization parameter $\alpha > 0$ the functional \mathcal{G}_α in (10) is well posed in the generalized sense of definition 1.

Theorem 5 (Well-Posedness). *Let the assumptions of proposition 4 and the general assumption of this paper hold. The functional \mathcal{G}_α in (10) attains generalized minimizers on the set of admissible quintuples.*

Sketch of the proof. It follows from remark 3 that the set of admissible quintuples is not empty. Thus, there exists a minimizing sequence of admissible quintuples for $\hat{\mathcal{G}}_\alpha$. It follows from the coercivity of ρ in lemma 3, the Sobolev compact embedding of H^1 into L^2 [1], and the compact embedding of BV into L^1 [15], that this minimizing sequence converges to some quintuple which is admissible (see lemma 2). Next, from the weak lower semi-continuity of ρ , together with the continuity of F_j (see proposition 4), and the continuity of q (see lemma 1), we conclude that this limit quintuple is a minimizer of $\hat{\mathcal{G}}_\alpha$. \square

In the next two theorems we present the main convergence and stability results. The proofs use classical techniques from the analysis of Tikhonov type regularization methods (see, e.g. [10]).

Theorem 6 (Convergence for exact data). *Assume we have exact data (i.e. $\gamma_j^\delta = \gamma_j$) and let $(z_\alpha^1, z_\alpha^2, z_\alpha^3, \varphi_\alpha, \psi_\alpha)$, $\alpha > 0$, denote a generalized minimizer of $\hat{\mathcal{G}}_\alpha$. Then, for every sequence of positive numbers $\{\alpha_k\}_{k \in \mathbb{N}}$ converging to zero there exists a subsequence (denoted again by $\{\alpha_k\}$) such that $(z_{\alpha_k}^1, z_{\alpha_k}^2, z_{\alpha_k}^3, \varphi_{\alpha_k}, \psi_{\alpha_k})$ is strongly convergent in $(L^1(\Omega))^3 \times (L^2(\Omega))^2$ to some $(\bar{z}^1, \bar{z}^2, \bar{z}^3, \bar{\varphi}, \bar{\psi})$. Moreover, the limit is a solution of $F_j(q(\bar{z}^1, \bar{z}^2, \bar{z}^3)) = \gamma_j$, $j = 1, \dots, N$.*

Sketch of the proof. Let $\{\alpha_k\}_{k \in \mathbb{N}}$ satisfy the above assumptions. For each $k \in \mathbb{N}$, we denote by $(z_k^1, z_k^2, z_k^3, \varphi_k, \psi_k) := (z_{\alpha_k}^1, z_{\alpha_k}^2, z_{\alpha_k}^3, \varphi_{\alpha_k}, \psi_{\alpha_k})$ a minimizer of G_{α_k} (that exists by theorem 5). It follows from Assumption (A2) that

$$\begin{aligned} G_{\alpha_k}(z_k^1, z_k^2, \varphi_k, \psi_k) &\leq \sum_{j=1}^N \|F_j(q(z^1, z^2, z^3)) - \gamma_j\| + \alpha_k \rho(z^1, z^2, z^3 \varphi^*, \psi^*) \\ &= \alpha_k \rho(z^1, z^2, z^3 \varphi^*, \psi^*), \quad k \in \mathbb{N}. \end{aligned} \quad (15)$$

As a consequence of (15) we obtain

$$\rho(z_k^1, z_k^2, z_k^3, \varphi_k, \psi_k) \leq \rho(z^1, z^2, z^3 \varphi^*, \psi^*) < \infty. \quad (16)$$

Then, arguing with (16) and lemma 3, we prove that the sequences $\{\varphi_k\}$, $\{\psi_k\}$ and $\{z_k^j\}$ are bounded in $H^1(\Omega)$ and BV respectively.

Arguing as in theorem 5, we conclude the existence of strong converging subsequences, with limit $(\bar{z}^1, \bar{z}^2, \bar{z}^3, \bar{\varphi}, \bar{\psi})$ being an admissible quintuple. Moreover, from lemma 1 (a), the continuity of F_j (see proposition 4), the assumption on the sequence $\{\alpha_k\}$, and (15) we obtain

$$\gamma_j = \lim_{k \rightarrow \infty} F_j(q(z_k^1, z_k^2, z_k^3)) = F_j(q(\bar{z}^1, \bar{z}^2, \bar{z}^3)),$$

concluding the proof. \square

Theorem 7 (Convergence for noisy data). *Let $\alpha = \alpha(\delta)$ be a function satisfying $\lim_{\delta \rightarrow 0} \alpha(\delta) = 0$ and $\lim_{\delta \rightarrow 0} \delta^2 \alpha(\delta)^{-1} = 0$. Moreover, let $\{\delta_k\}_{k \in \mathbb{N}}$ be a sequence of positive numbers converging to zero and $\gamma^{\delta_k} \in Y$ be corresponding noisy data satisfying (3). Then there exists a subsequence, again denoted by $\{\delta_k\}$, and a sequence $\{\alpha_k := \alpha(\delta_k)\}$ such that*

$(z_{\alpha_k}^1, z_{\alpha_k}^2, z_{\alpha_k}^3, \varphi_{\alpha_k}, \psi_{\alpha_k})$ converges in $(L^1(\Omega))^3 \times (L^2(\Omega))^2$ to some $(\bar{z}^1, \bar{z}^2, \bar{z}^3, \bar{\varphi}, \bar{\psi})$ satisfying $F_j(q(\bar{z}^1, \bar{z}^2, \bar{z}^3)) = \gamma_j, j = 1, \dots, N$.

Sketch of the proof. For each $k \in \mathbb{N}$, let $\{\alpha_k\}_{k \in \mathbb{N}} := \{\alpha_k(\delta_k)\}_{k \in \mathbb{N}}$ and the corresponding $(z_k^1, z_k^2, z_k^3, \varphi_k, \psi_k) := (z_{\alpha_k(\delta_k)}^1, z_{\alpha_k(\delta_k)}^2, z_{\alpha_k(\delta_k)}^3, \varphi_{\alpha_k(\delta_k)}, \psi_{\alpha_k(\delta_k)})$ be a minimizer of G_{α_k} (that exists by theorem 5). It follows from Assumption (A2) that

$$\begin{aligned} G_{\alpha_k(\delta_k)}(z_k^1, z_k^2, \varphi_k, \psi_k) &\leq \sum_{j=1}^N \left\| F_j(q(z^1, z^2, z^3)) - \gamma_j^{\delta_k} \right\|^2 + \alpha_k \rho(z^1, z^2, z^3 \varphi^*, \psi^*) \\ &\leq N \delta_k^2 + \alpha_k \rho(z^1, z^2, z^3 \varphi^*, \psi^*), k \in \mathbb{N}. \end{aligned} \quad (17)$$

From (17) and the assumptions on $\{\alpha_k\}$, it follows that $\{\rho(z_k^1, z_k^2, z_k^3, \varphi_k, \psi_k)\}$ is bounded. From this fact and lemma 3, we conclude that $\{\varphi_k\}$, $\{\psi_k\}$ and $\{z_k^j\}$ are bounded in $H^1(\Omega)$ and BV respectively. To conclude the proof, it is enough to argue as in the last paragraph of the proof of theorem 6. \square

3.3. Proof of proposition 4

In the proof of proposition 4, a result of L^p -regularity for the solution of elliptic boundary value problems of Neumann type is needed. Such regularity is obtained by a modification of a result by Meyers [30], which guarantee $W^{1,p}$ -regularity of u^* (the solution of (1)), provided $b^* \in \mathcal{V}$. For details, we refer the reader to [18].

Lemma 8 (Meyers). *Let $\Omega \subset \mathbb{R}^2$ be a bounded connected domain with Lipschitz boundary, $b \in \mathcal{V}$ and $u \in H^1(\Omega)$ be the unique solution of (1).*

There exists a constant $p_0 \in (2, \infty)$ depending only on b_i, b_e and Ω , such that for every $p \in (2, p_0)$ and $s \in [p/2, \infty]$, there exists a constant $C = C(p, s, b_i, b_e, \Omega)$ such that

$$\|u\|_{W^{1,p}(\Omega)} \leq C \|\eta_j\|_{L^s(\partial\Omega)},$$

whenever η_j has the extra regularity $\eta_j \in (W^{1-1/q,q}(\partial\Omega))'$, for $q^{-1} + p^{-1} = s^{-1}$.

The constant p_0 in proposition 4 is chosen as in lemma 8. Next, we introduce some notation and the necessary assumptions on the smoothness of the boundary data in (1). Let $b \in \mathcal{V}$ be given as in (7), and assume that the current profile η_j in the BVP (1) satisfies⁵ the assumption of proposition 4.

Now, for each $j \in \{1, \dots, N\}$, consider the operator $G_j : V \subset X \rightarrow H^1(\Omega)$ given by $G_j(b) = u_j$, where $u_j \in H^1(\Omega)$ is the unique solution of (1) in $H_*^1(\Omega) := \{w \in H^1(\Omega) : \int_{\partial\Omega} w = 0\}$. Thus the operator F_j in (2) satisfies $F_j(b) = \Gamma_D(G_j(b))$, where $\Gamma_D : H^1(\Omega) \rightarrow H^{1/2}(\partial\Omega)$ is the Dirichlet trace operator, which is linear and continuous [1]. Consequently, in order to prove the continuity of F_j stated in proposition 4 at some point $b^* \in \mathcal{V}$, it is sufficient to verify the estimate

$$\|G_j(b) - G_j(b^*)\|_{H^1(\Omega)} \leq C^* \|b - b^*\|_{L^1(\Omega)}^{1/p} \quad (18)$$

for some constant $C^* > 0$ depending only on b^* and some $p > 2$, as in lemma 8.

In what follows, we denote (for simplicity) $u := G_j(b)$ and $u^* := G_j(b^*)$. Using integration by parts, we obtain

⁵ Note that, under the hypothesis of proposition 4, we have $(W^{1-1/q,q}(\partial\Omega))' \subset H^{-1/2}(\partial\Omega)$.

$$\begin{aligned}
\int_{\Omega} b |\nabla(u^* - u)|^2 &= \int_{\Omega} b |\nabla u^*|^2 - 2 \int_{\partial\Omega} b(u)_{\nu} u^* + \int_{\Omega} b |\nabla u|^2 \\
&= \int_{\Omega} (b - b^*) |\nabla u^*|^2 - \int_{\Omega} b^* |\nabla u^*|^2 + \int_{\Omega} b |\nabla u|^2 \\
&= \int_{\Omega} (b - b^*) |\nabla u^*|^2 - \int_{\partial\Omega} b^* (u^*)_{\nu} u^* + \int_{\partial\Omega} b(u)_{\nu} u \\
&= \int_{\Omega} (b - b^*) |\nabla u^*|^2 - \int_{\Omega} b \nabla u \nabla u^* + \int_{\Omega} b^* \nabla u^* \nabla u \\
&= \int_{\Omega} (b - b^*) |\nabla u^*|^2 - \int_{\Omega} (b - b^*) \nabla u^* \nabla u \\
&= \int_{\Omega} (b - b^*) \nabla u^* (\nabla u^* - \nabla u).
\end{aligned} \tag{19}$$

Since $b \in \mathcal{V}$ (see (7)), it follows from the Hölder inequality

$$b_i \int_{\Omega} |\nabla(u^* - u)|^2 \leq \left(\int_{\Omega} |b - b^*|^q \right)^{\frac{1}{q}} \left(\int_{\Omega} |\nabla u^*|^p \right)^{\frac{1}{p}} \left(\int_{\Omega} |\nabla(u^* - u)|^r \right)^{\frac{1}{r}} \tag{20}$$

for $p, q, r > 1$ with $\frac{1}{p} + \frac{1}{q} + \frac{1}{r} = 1$. Choosing $r = 2$ in (20), we obtain

$$b_i \left(\int_{\Omega} |\nabla(u^* - u)|^2 \right)^{\frac{1}{2}} \leq \left(\int_{\Omega} |b - b^*|^q \right)^{\frac{1}{q}} \left(\int_{\Omega} |\nabla u^*|^p \right)^{\frac{1}{p}}, \tag{21}$$

for $p, q > 1$ with $\frac{1}{p} + \frac{1}{q} = \frac{1}{2}$. From the L^p -regularity result in lemma 8, it follows the existence of $p_0 > 2$ such that $\|\nabla u^*\|_{L^p} < \infty$ for $2 < p \leq p_0$. Thus, choosing $p = 2 + \epsilon$ and $q = p/(p - 2) = (2\epsilon + 4)/\epsilon$ in (21), we conclude that

$$\|\nabla u^* - \nabla u\|_{L^2} \leq b_i^{-1} \|\nabla u^*\|_{L^p} \|b - b^*\|_{L^q}.$$

Consequently, we get the estimate

$$\|G_j(b) - G_j(b^*)\|_{H^1} \leq (c_P b_i)^{-1} \|\nabla u^*\|_{L^p} \|b - b^*\|_{L^q}, \tag{22}$$

where $c_P = c_P(\Omega)$ is the constant in the Poincaré inequality with null mean [1].

Moreover, since $q > 2$, we can write $q = 1 + \bar{q}$ (with $\bar{q} > 1$) and estimate the last term in (22) by

$$\|b - b^*\|_{L^q} = \left(\int_{\Omega} |b - b^*| |b - b^*|^{\bar{q}} \right)^{1/q} \leq (2b_e)^{\bar{q}/q} \|b - b^*\|_{L^1}^{1/q} \tag{23}$$

(notice that $b, b^* \in \mathcal{V}$ implies $|b - b^*| \leq 2b_e$ a.e. in Ω). Finally, from (22) and (23) follows (18) with $q = (2\epsilon + 4)/\epsilon$ and $C^* = C^*(u^*) = (c_P b_i)^{-1} \|\nabla u^*\|_{L^p} (2b_e)^{\bar{q}/q}$, where $p = 2 + \epsilon$. \square

4. Towards numerical realization

The Tikhonov functional \mathcal{G}_{α} defined in the previous section is not suitable for computing numerical approximations to the solution of (9). This becomes obvious when one observes the definition of the penalization term ρ in (13). In this section we introduce the functional $\mathcal{G}_{\varepsilon, \alpha}$, which can be used for the purpose of numerical implementations. This functional is defined in such a way that its minimizers are ‘close’ to the generalized minimizers of \mathcal{G}_{α} in a sense that will be made clear later (see proposition 9). For each $\varepsilon > 0$ we define the functional

$$\begin{aligned} \mathcal{G}_{\varepsilon,\alpha}(\varphi, \psi) := & \sum_{j=1}^N \|F_j(P_\varepsilon(\varphi, \psi)) - \gamma_j^\delta\|_Y^2 + \alpha(\mu_1|H_\varepsilon(\varphi + \beta/2)|_{\text{BV}} + \mu_2|H_\varepsilon(\varphi - \beta/2)|_{\text{BV}} \\ & + \mu_3|H_\varepsilon(\psi)|_{\text{BV}} + \mu_4\|\varphi - \varphi_0\|_{H^1}^2 + \mu_5\|\psi - \psi_0\|_{H^1}^2), \end{aligned} \quad (24)$$

where $P_\varepsilon(\varphi, \psi) := q(H_\varepsilon(\varphi + \beta/2), H_\varepsilon(\varphi - \beta/2), H_\varepsilon(\psi))$ is the functional defined in (11). In the next proposition we verify that this functional is well-posed. Moreover, we prove that, for $\varepsilon \rightarrow 0$, the minimizers of $\mathcal{G}_{\varepsilon,\alpha}$ approximate a generalized minimizer of \mathcal{G}_α . The proof follows the lines of [10, lemma 10 and theorem 11]. For the convenience of the reader, a sketch of the proof is presented.

Proposition 9. *Let $\alpha, \beta, \varepsilon > 0$ and $\varphi_0, \psi_0 \in H^1(\Omega)$ be given. Then*

- (a) *The functional $\mathcal{G}_{\varepsilon,\alpha}$ in (24) attains a minimizer on $(H^1(\Omega))^2$.*
 (b) *For each $\varepsilon > 0$ denote by $(\varphi_{\varepsilon,\alpha}, \psi_{\varepsilon,\alpha})$ a minimizer of $\mathcal{G}_{\varepsilon,\alpha}$. There exists a positive sequence $\{\varepsilon_k\}$ converging to zero such that $(H_{\varepsilon_k}(\varphi_{\varepsilon_k,\alpha} + \frac{\beta}{2}), H_{\varepsilon_k}(\varphi_{\varepsilon_k,\alpha} - \frac{\beta}{2}), H_{\varepsilon_k}(\psi_{\varepsilon_k,\alpha}), \varphi_{\varepsilon_k,\alpha}, \psi_{\varepsilon_k,\alpha})$ converges strongly in $(L^1(\Omega))^3 \times (L^2(\Omega))^2$ and the limit is a generalized minimizer of \mathcal{G}_α in the set of admissible quintuples.*

Proof. Sketch of the proof Since $\varepsilon > 0, \alpha > 0$, and $\inf\{\mathcal{G}_{\varepsilon,\alpha}(\varphi, \psi) : (\varphi, \psi) \in (H^1(\Omega))^2\} \leq \mathcal{G}_{\varepsilon,\alpha}(0, 0) < \infty$, there exists a minimizing sequence $\{(\varphi_k, \psi_k)\}_{k \in \mathbb{N}}$ for $\mathcal{G}_{\varepsilon,\alpha}$. The definition of $\mathcal{G}_{\varepsilon,\alpha}$, implies that the minimizing sequence $\{(\varphi_k, \psi_k)\}_{k \in \mathbb{N}}$ is bounded in $(H^1(\Omega))^2$. Then, the compact embedding theorem [1, chapter 5] and lemma 1 imply the existence of a subsequence (denoted with the same index) such that $(\varphi_k, \psi_k) \rightarrow (\varphi, \psi)$ in $(L^2(\Omega))^2$, $P_\varepsilon(\varphi_k, \psi_k) \rightarrow P_\varepsilon(\varphi, \psi)$ in $L^1(\Omega)$, $H_\varepsilon(\varphi_k \pm \frac{\beta}{2}) \rightarrow H_\varepsilon(\varphi \pm \frac{\beta}{2})$ and $H_\varepsilon(\psi_k) \rightarrow H_\varepsilon(\psi)$ in $L^1(\Omega)$.

Furthermore, from the weak lower semi-continuity of the BV-seminorm [15, theorem 1, p 172] and of the H^1 -norm, we obtain $|H_\varepsilon(\varphi \pm \frac{\beta}{2})|_{\text{BV}} \leq \liminf_{k \rightarrow \infty} |H_\varepsilon(\varphi_k \pm \frac{\beta}{2})|_{\text{BV}}$, $|H_\varepsilon(\psi)|_{\text{BV}} \leq \liminf_{k \rightarrow \infty} |H_\varepsilon(\psi_k)|_{\text{BV}}$, $\|\varphi - \varphi_0\|_{H^1(\Omega)}^2 \leq \liminf_{k \rightarrow \infty} \|\varphi_k - \varphi_0\|_{H^1(\Omega)}^2$, $\|\psi - \psi_0\|_{H^1(\Omega)}^2 \leq \liminf_{k \rightarrow \infty} \|\psi_k - \psi_0\|_{H^1(\Omega)}^2$. These facts together with the continuity of both F_j and q (see proposition 4 and lemma 1) allow us to conclude that $\mathcal{G}_{\varepsilon,\alpha}(\varphi, \psi) \leq \liminf_{k \rightarrow \infty} \mathcal{G}_{\varepsilon,\alpha}(\varphi_k, \psi_k) = \inf_{k \rightarrow \infty} \mathcal{G}_{\varepsilon,\alpha}$, proving Assertion (a).

Add Assertion (b).

Let $(z_\alpha^1, z_\alpha^2, z_\alpha^3, \varphi_\alpha, \psi_\alpha)$ be an admissible quintuple minimizing $\hat{\mathcal{G}}_\alpha$ (that exists by theorem 5). From definition 1 follows the existence of a positive sequence $\varepsilon_k \rightarrow 0$ and a corresponding sequence $(\varphi_k, \psi_k) \in (H^1(\Omega))^2$ such that

$$(\varphi_k, \psi_k, H_{\varepsilon_k}(\varphi_k + \frac{\beta}{2}), H_{\varepsilon_k}(\varphi_k - \frac{\beta}{2}), H_{\varepsilon_k}(\psi_k)) \rightarrow (\varphi_\alpha, \psi_\alpha, z_\alpha^1, z_\alpha^2, z_\alpha^3)$$

in $(L^2(\Omega))^2 \times (L^1(\Omega))^3$ as $k \rightarrow \infty$. Moreover, from lemma 3 we can further assume that $\rho(z_\alpha^1, z_\alpha^2, z_\alpha^3, \varphi_\alpha, \psi_\alpha) = \lim_{k \rightarrow \infty} (\mu_1|H_{\varepsilon_k}(\varphi_k + \frac{\beta}{2})|_{\text{BV}} + \mu_2|H_{\varepsilon_k}(\varphi_k - \frac{\beta}{2})|_{\text{BV}} + \mu_3|H_{\varepsilon_k}(\psi_k)|_{\text{BV}} + \mu_4\|\varphi_k - \varphi_0\|_{H^1}^2 + \mu_5\|\psi_k - \psi_0\|_{H^1}^2)$.

Let $(\varphi_{\varepsilon_k}, \psi_{\varepsilon_k})$ be a minimizer of $\mathcal{G}_{\varepsilon_k,\alpha}$, for each $k \in \mathbb{N}$. From the definition of $\mathcal{G}_{\varepsilon_k,\alpha}$ follows that each coordinate of the sequence $\{(\|\varphi_{\varepsilon_k} - \varphi_0\|_{H^1}, \|\psi_{\varepsilon_k} - \psi_0\|_{H^1}, |H_{\varepsilon_k}(\varphi_{\varepsilon_k} + \frac{\beta}{2})|_{\text{BV}}, |H_{\varepsilon_k}(\varphi_{\varepsilon_k} - \frac{\beta}{2})|_{\text{BV}}, |H_{\varepsilon_k}(\psi_{\varepsilon_k})|_{\text{BV}})\}_k$ is uniformly bounded by $\mathcal{G}_{\varepsilon_k,\alpha}(0, 0) < \infty$. Hence, from the compact embedding theorems for $H^1(\Omega)$ in $L^2(\Omega)$, and for BV in $L^1(\Omega)$, we conclude the existence of subsequences (again denoted by the same indexes) such that

$$(\varphi_{\varepsilon_k}, \psi_{\varepsilon_k}, H_{\varepsilon_k}(\varphi_{\varepsilon_k} + \frac{\beta}{2}), H_{\varepsilon_k}(\varphi_{\varepsilon_k} - \frac{\beta}{2}), H_{\varepsilon_k}(\psi_{\varepsilon_k})) \rightarrow (\hat{\varphi}, \hat{\psi}, \hat{z}^1, \hat{z}^2, \hat{z}^3)$$

in $(L^2(\Omega))^2 \times L^1((\Omega))^3$ as $k \rightarrow \infty$. This characterizes the limit $(\hat{\varphi}, \hat{\psi}, \hat{z}^1, \hat{z}^2, \hat{z}^3)$ as an admissible quintuple (see definition 1). Now, the continuity of F_j and q (see proposition 4 and lemma 1) and the characterization of ρ as a Γ -limit (see lemma 3) implies that $\|F_j(q(\hat{z}^1, \hat{z}^2, \hat{z}^3)) - \gamma_j^\delta\| = \lim_{k \rightarrow \infty} \|F_j(P_{\varepsilon_k}(\varphi_{\varepsilon_k}, \psi_{\varepsilon_k})) - \gamma_j^\delta\|$ and

$$\begin{aligned} \rho(\hat{z}^1, \hat{z}^2, \hat{z}^3, \hat{\varphi}, \hat{\psi}) &\leq \liminf_{k \rightarrow \infty} (\mu_1 |H_{\varepsilon_k}(\varphi_{\varepsilon_k} + \frac{\beta}{2})|_{\text{BV}} + \mu_2 |H_{\varepsilon_k}(\varphi_{\varepsilon_k} - \frac{\beta}{2})|_{\text{BV}} \\ &\quad + \mu_3 |H_{\varepsilon_k}(\psi_{\varepsilon_k})|_{\text{BV}} + \mu_4 \|\varphi_{\varepsilon_k} - \varphi_0\|_{H^1}^2 + \mu_5 \|\psi_{\varepsilon_k} - \psi_0\|_{H^1}^2). \end{aligned}$$

Thus,

$$\begin{aligned} \mathcal{G}_\alpha(\hat{z}^1, \hat{z}^2, \hat{z}^3, \hat{\varphi}, \hat{\psi}) &= \sum_{j=1}^N \|F_j(q(\hat{z}^1, \hat{z}^2, \hat{z}^3)) - \gamma_j^\delta\|^2 + \alpha \rho(\hat{z}^1, \hat{z}^2, \hat{z}^3, \hat{\varphi}, \hat{\psi}) \\ &\leq \liminf_{k \rightarrow \infty} \mathcal{G}_{\varepsilon_k, \alpha}(\varphi_{\varepsilon_k}, \psi_{\varepsilon_k}) \\ &\leq \liminf_{k \rightarrow \infty} \mathcal{G}_{\varepsilon_k, \alpha}(\varphi_k, \psi_k) \leq \limsup_{k \rightarrow \infty} \mathcal{G}_{\varepsilon_k, \alpha}(\varphi_k, \psi_k) \\ &\leq \sum_{j=1}^N \limsup_{k \rightarrow \infty} \|F_j(P_{\varepsilon_k}(\varphi_k, \psi_k)) - \gamma_j^\delta\|^2 + \alpha \limsup_{k \rightarrow \infty} (\mu_1 |H_{\varepsilon_k}(\varphi_k + \frac{\beta}{2})|_{\text{BV}} \\ &\quad + \mu_2 |H_{\varepsilon_k}(\varphi_k - \frac{\beta}{2})|_{\text{BV}} + \mu_3 |H_{\varepsilon_k}(\psi_k)|_{\text{BV}} + \mu_4 \|\varphi_k - \varphi_0\|_{H^1}^2 + \mu_5 \|\psi_k - \psi_0\|_{H^1}^2) \\ &= \sum_{j=1}^N \|F_j(q(z_\alpha^1, z_\alpha^2, z_\alpha^3)) - \gamma_j^\delta\|^2 + \alpha \rho(z_\alpha^1, z_\alpha^2, z_\alpha^3, \varphi_\alpha, \psi_\alpha) = \inf \hat{\mathcal{G}}_\alpha, \end{aligned}$$

proving that $(\hat{z}^1, \hat{z}^2, \hat{z}^3, \hat{\varphi}, \hat{\psi})$ is a minimizer of \mathcal{G}_α . \square

Proposition 9 justifies the use functionals $\mathcal{G}_{\varepsilon, \alpha}$ in order to obtain numerical approximations to the generalized minimizers of \mathcal{G}_α . It is worth noticing that, differently from \mathcal{G}_α , the minimizers of $\mathcal{G}_{\varepsilon, \alpha}$ can be numerically computed. In the next subsection we compute the first order conditions of optimality for the functional $\mathcal{G}_{\varepsilon, \alpha}$, which will allow us to compute the desired minimizers.

4.1. Optimality conditions for the Tikhonov functional

For the numerical purposes we have in mind, it is necessary to derive the first order optimality conditions for a minimizer of the functionals $\mathcal{G}_{\varepsilon, \alpha}$. To this end we consider $\mathcal{G}_{\varepsilon, \alpha}$ in (24) and we look for the Gâteaux directional derivatives with respect to φ, ψ .

Since $H'_\varepsilon(\varphi \pm \beta/2)$ and $H'_\varepsilon(\psi)$ are self-adjoint⁶, the optimality conditions for a minimizer of the functional $\mathcal{G}_{\varepsilon, \alpha}$ can be written in the form of the system of equations

$$\alpha \mu_4 (I - \Delta)(\varphi - \varphi_0) = -R_{\varepsilon, \alpha}^1(\varphi, \psi), \quad \alpha \mu_5 (I - \Delta)(\psi - \psi_0) = -R_{\varepsilon, \alpha}^2(\varphi, \psi), \quad \text{in } \Omega \quad (25a)$$

$$(\varphi - \varphi_0)_\nu = 0, \quad (\psi - \psi_0)_\nu = 0, \quad \text{at } \partial\Omega \quad (25b)$$

where $\nu(x)$ is the external unit normal vector at $x \in \partial\Omega$, and

⁶ Notice that $H'_\varepsilon(t) = \begin{cases} 1/\varepsilon & t \in (-\varepsilon, 0) \\ 0 & \text{else} \end{cases}$.

$$\begin{aligned}
R_{\varepsilon,\alpha}^1(\varphi, \psi) = & \sum_{j=1}^N (b_i - b_e) H_\varepsilon(\psi) H'_{\beta,\varepsilon}(\varphi) F'_j(P_\varepsilon(\varphi, \psi))^* (F_j(P_\varepsilon(\varphi, \psi)) - \gamma_j^\delta) \\
& - \frac{\alpha}{2} \left[\mu_1 H'_\varepsilon(\varphi + \frac{\beta}{2}) \nabla \cdot \left(\frac{\nabla H_\varepsilon(\varphi + \frac{\beta}{2})}{|\nabla H_\varepsilon(\varphi + \frac{\beta}{2})|} \right) \right. \\
& \left. + \mu_2 H'_\varepsilon(\varphi - \frac{\beta}{2}) \nabla \cdot \left(\frac{\nabla H_\varepsilon(\varphi - \frac{\beta}{2})}{|\nabla H_\varepsilon(\varphi - \frac{\beta}{2})|} \right) \right], \quad (26a)
\end{aligned}$$

$$\begin{aligned}
R_{\varepsilon,\alpha}^2(\varphi, \psi) = & \sum_{j=1}^N (b_i - b_e) H_{\beta,\varepsilon}(\varphi) H'_\varepsilon(\psi) F'_j(P_\varepsilon(\varphi, \psi))^* (F_j(P_\varepsilon(\varphi, \psi)) - \gamma_j^\delta) \\
& - \frac{\alpha}{2} \mu_3 H'_\varepsilon(\psi) \nabla \cdot \left(\frac{\nabla H_\varepsilon(\psi)}{|\nabla H_\varepsilon(\psi)|} \right). \quad (26b)
\end{aligned}$$

It is worth noticing that the derivation of (25) is purely heuristic, since the BV seminorm is not differentiable. Moreover, due to the terms $|\nabla H_\varepsilon(\cdot)|$, $|\nabla H_\varepsilon(\cdot \pm \frac{\beta}{2})|$ appearing in the denominators of (26), we have to assume that the gradients $\nabla \varphi$, $\nabla \psi$ do not vanish in a ε -neighborhood of the level curves $\{\varphi = \frac{\beta}{2}\}$, $\{\varphi = -\frac{\beta}{2}\}$ and $\{\psi = 0\}$ respectively (compare with assumption (A2)).

In what follows we apply iterative regularization to the system of optimality conditions (25). This idea was suggested in [10] and allow the derivation of an iterative regularization method on the space of parameters modeled by level-set functions. The resulting method is the starting point of the iterative algorithm proposed in this article for solving the crack detection problem (see section 5).

4.2. An iterative regularization method

The method discussed in the sequel consists of successively solving the system of optimality conditions in (25). This regularization method was used in connection with level-set approaches in [10, 17].

For $n = 0$ set $\mathcal{G}_{\varepsilon,\alpha}^{(0)}(\varphi, \psi) := \mathcal{G}_{\varepsilon,\alpha}(\varphi, \psi)$ as in (24), where (φ_0, ψ_0) is some initial guess. The iterative regularization method under consideration consists in minimizing the family of functionals

$$\begin{aligned}
\mathcal{G}_{\varepsilon,\alpha}^{(n)}(\varphi, \psi) := & \sum_{j=1}^N \|F_j(P_\varepsilon(\varphi, \psi)) - \gamma_j^\delta\|_Y^2 + \alpha \left(\mu_1 |H_\varepsilon(\varphi + \frac{\beta}{2})|_{\text{BV}} + \mu_2 |H_\varepsilon(\varphi - \frac{\beta}{2})|_{\text{BV}} \right. \\
& \left. + \mu_3 |H_\varepsilon(\psi)|_{\text{BV}} + \mu_4 \|\varphi - \varphi_n\|_{H^1}^2 + \mu_5 \|\psi - \psi_n\|_{H^1}^2 \right). \quad (27)
\end{aligned}$$

The minimizer of $\mathcal{G}_{\varepsilon,\alpha}^{(n)}(\varphi, \psi)$ is denoted by $(\varphi_{n+1}, \psi_{n+1})$. Notice that $(\varphi_{n+1}, \psi_{n+1})$ can be realized by solving the system of optimality conditions

$$\begin{aligned}
\alpha \mu_4 (I - \Delta)(\varphi - \varphi_n) &= -R_{\varepsilon,\alpha}^1(\varphi, \psi), & \alpha \mu_5 (I - \Delta)(\psi - \psi_n) &= -R_{\varepsilon,\alpha}^2(\varphi, \psi), & \text{in } \Omega \\
(\varphi - \varphi_n)_\nu &= 0, & (\psi - \psi_n)_\nu &= 0, & \text{at } \partial\Omega.
\end{aligned}$$

In the sequel we describe an algorithm (see algorithm 1) to implement the iterative regularization method for the crack identification problem. Each iteration of this algorithm consists of four steps:

Algorithm 1. Iterative regularization method for solving the crack detection problem.

1. Evaluate $[r_j]_{j=1}^N := [F_j(P_\varepsilon(\varphi_n, \psi_n)) - \gamma_j^\delta]_{j=1}^N = [w_j]_{\partial\Omega} - \gamma_j^\delta]_{j=1}^N$,
where $[w_j]_{j=1}^N \in [H^1(\Omega)]^N$ solves

$$\nabla \cdot (P_\varepsilon(\varphi_n, \psi_n) \nabla w_j) = 0, \text{ in } \Omega; \quad b(w_j)_\nu = \eta_j, \text{ at } \partial\Omega.$$
 2. Evaluate $[F_j'(P_\varepsilon(\varphi_n, \psi_n)) * r_j]_{j=1}^N := -[\nabla w_j \cdot \nabla u_j]_{j=1}^N \in [L^2(\Omega)]^N$, where $[w_j]_{j=1}^N$ is the
function computed in Step 1. and $[u_j]_{j=1}^N \in [H^1(\Omega)]^N$ solves

$$\nabla \cdot (P_\varepsilon(\varphi_n, \psi_n) \nabla u_j) = 0 \text{ in } \Omega; \quad b(u_j)_\nu = r_j, \text{ at } \partial\Omega.$$
 3. Calculate $R_{\varepsilon, \alpha}^1(\varphi_n, \psi_n)$ and $R_{\varepsilon, \alpha}^2(\varphi_n, \psi_n)$ as in (26).
 4. Evaluate the updates $\delta\varphi, \delta\psi \in H^1(\Omega)$ by solving

$$\alpha\mu_4(I - \Delta)\delta\varphi = -R_{\varepsilon, \alpha}^1(\varphi_n, \psi_n), \text{ in } \Omega; \quad (\delta\varphi)_\nu = 0, \text{ at } \partial\Omega.$$

$$\alpha\mu_5(I - \Delta)\delta\psi = -R_{\varepsilon, \alpha}^2(\varphi_n, \psi_n), \text{ in } \Omega; \quad (\delta\psi)_\nu = 0, \text{ at } \partial\Omega.$$
 5. Update the level-set functions $\varphi_{n+1} = \varphi_n + \delta\varphi, \psi_{n+1} = \psi_n + \delta\psi$.
-

- In the first step the residual $[r_j]_{j=1}^N \in [L^2(\partial\Omega)]^N$ corresponding to the iterate (φ_n, ψ_n) is evaluated. This requires the solution of N elliptic BVP's of Neumann type.
- In the second step the solutions $[u_j]_{j=1}^N \in H^1(\Omega)$ of the adjoint problems for the residual components $[r_j]_{j=1}^N$ are evaluated. This corresponds to solving N elliptic BVP of Neumann type and to computing N inner product in L^2 (namely $[\nabla w_j \cdot \nabla u_j]_{j=1}^N$).
- The third step consists in the computation of $R_{\varepsilon, \alpha}^1(\varphi_n, \psi_n)$ and $R_{\varepsilon, \alpha}^2(\varphi_n, \psi_n)$. Each computation requires the sum of N inner products in L^2 .
- In the fourth step, the updates $\delta\varphi_n, \delta\psi_n \in H^1(\Omega)$ for the level-set functions φ_n and ψ_n are evaluated. This corresponds to solving two non-coupled elliptic BVP's of Neumann type.

Remark 5. In section 4.2 we propose an iterative method (summarized in algorithm 1) to compute approximate solutions of the system of operator equation (9). The method under consideration is the 'iterated Tikhonov method' given by

$$(\varphi_{n+1}, \psi_{n+1}) := \arg \min_{\varphi, \psi} \mathcal{G}_{\varepsilon, \alpha}^{(n)}(\varphi, \psi), n = 0, 1, \dots$$

where the functionals $\mathcal{G}_{\varepsilon, \alpha}^{(n)}, n \in \mathbb{N}$ are defined in (27). Notice that $(\varphi_{n+1}, \psi_{n+1})$ is the solution of optimality condition for $\mathcal{G}_{\varepsilon, \alpha}^{(n)}$ (see (25) and (26)).

A similar algorithm was successfully used in [10, 17] to solve the inverse potential problem under the framework of level-sets and multiple level-sets respectively. However, what concerns the crack detection problem the method outlined above becomes disadvantageous if the number of physical experiments N in (1) is large. Indeed, in each iteration one has to solve $2N + 2$ elliptic BVP's.

5. Numerical experiments

In this section we present reconstruction results obtained from a numerical implementation of the level-set method discussed in this manuscript (see algorithm 1).

In what follows $\Omega \subset \mathbb{R}^2$ is the unit disk. We address the identification of three distinct crack scenarios: the piecewise constant functions b_1^* (curved crack close to the boundary), b_2^* ('S' shaped crack far from the boundary), b_3^* (two straight cracks) shown in figure 1. The (constant) thickness of the cracks is $\beta = 0.04$, the background conductivity is $b_e = 1.0$ and the crack conductivity is $b_i = 0.01$ (see section 1).

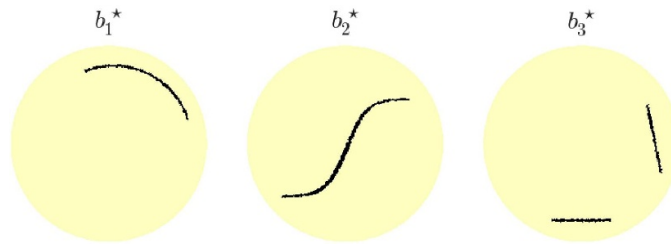


Figure 1. Exact cracks b_k^* , $k = 1, 2, 3$ used in the numerical experiments.

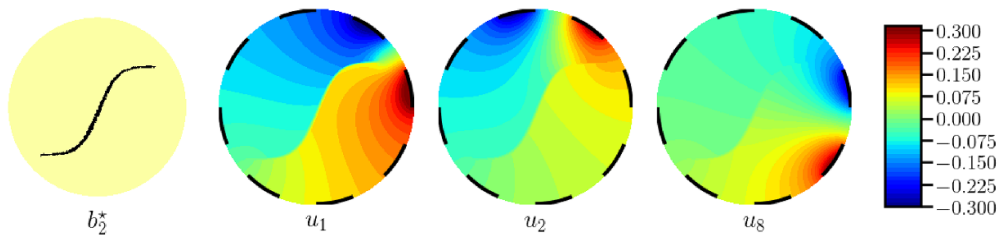


Figure 2. Typical Neumann-to-Dirichlet experiment. (LEFT) Crack b_2^* . (RIGHT) Solutions u_1 , u_2 and u_8 of (1) for the Neumann data η_1 , η_2 and η_8 respectively.

The solutions of the BVP's (required for the implementation of our method) are computed using a finite element type method and the open-source package FEniCS [2].

Remark 6. Since the conductivities are assumed to be known, these crack identification problems belong to the family of 'shape identification problems'.

When the conductivities are not known, we face a problem of simultaneous identification of 'shape and contrast'. This is known to be a challenging problem. In this case, it is possible to modify the Tikhonov functional in (10), in order to also determine the conductivity values (see, e.g. [11, section 1.3]).

5.1. Neumann/Dirichlet data

We use $N = 8$ distinct pairs of Neumann/Dirichlet boundary data $\{(\eta_j, \gamma_j)\}_{j=1}^N$ corresponding to 8 uniformly spaced electrodes placed around $\partial\Omega = \{x \in \mathbb{R}^2; \|x\| = 1\}$ (see figure 2 for a typical NtD experiment in the crack scenario b_2^*). Each Neumann data η_j is a piecewise constant function that takes current values 1 over one electrode, -1 on the adjacent electrode and zero elsewhere (adjacent current pattern); moreover, it satisfies $\int_{\partial\Omega} \eta_j = 0$.

In order to generate the exact data, in each crack scenario the BVP's in (1) with Neumann data η_j , $j = 1, \dots, N$ are solved; the corresponding solutions are denoted by $u_j : \Omega \rightarrow \mathbb{R}$. The Dirichlet data γ_j , $j = 1, \dots, N$, are computed as the Dirichlet trace of u_j at $\partial\Omega$, i.e. $\gamma_j := u_j|_{\partial\Omega}$.

In order to generate the noisy data γ_j^δ used in our experiments, the exact Dirichlet data γ_j are perturbed by adding uniformly distributed random noise. Two distinct levels of noise are used, namely $\delta = 1\%$ and $\delta = 20\%$.

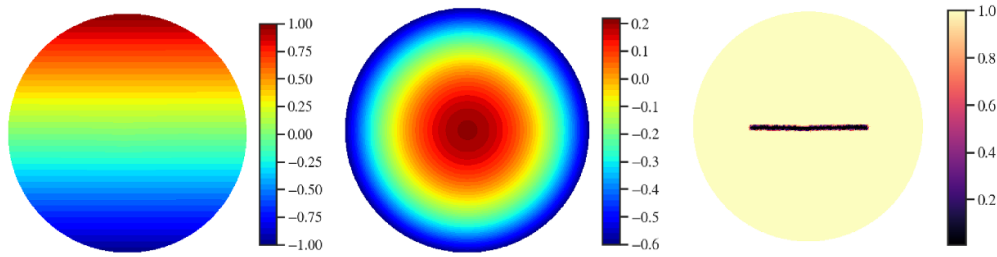


Figure 3. Initial guess for level-set functions φ_0 (LEFT), ψ_0 (CENTER), and the resulting crack $P_\varepsilon(\varphi_0, \psi_0)$ (RIGHT).

5.2. Relevant aspects of the numerical implementation

5.2.1. Initial guess and regularization parameters. The same initial guess is used in all numerical experiments. In figure 3 the initial guess for the level-set functions (φ_0, ψ_0) as well as the resulting crack $P_\varepsilon(\varphi_0, \psi_0)$ are depicted.

In all crack scenarios we use $\varepsilon = 0.01$ and $\mu_1 = \mu_2 = \mu_3 = 0.000001$, $\mu_4 = 1$. Moreover, $\mu_5 = 1$ in crack scenarios b_1^* , b_3^* , while $\mu_5 = 0.1$ in crack scenario b_2^* .

5.2.2. Meshes used in the numerical implementation. The solutions u_j of the BVP's in section 5.1 (needed to generate the data for the inverse problem) are computed using adaptively refined triangular meshes with average 40 000 elements (1200 boundary vertices).

In order to avoid inverse crimes, adaptively refined meshes (with average 11 000 elements and 600 boundary vertices) are used in the implementation of the level-set method (see algorithm 1). Notice that these meshes are coarser than the meshes used to generate the data for the inverse problem (see section 5.1).

A third uniform mesh with 18 182 elements and 600 boundary vertices is used to represent the level-set functions (φ_k, ψ_k) ; the same mesh is used for all steps k of the iterative method.

5.2.3. Reinitialization. We observed in the numerical implementation of our method that the level-set function φ_k develops small gradients as k grows large. This is a well known issue in level-set type methods, that leads to numerical instabilities. To address this difficulty, we implement a reinitialization type method [31]. The main purpose is to enforce the property $|\nabla \varphi_k| = 1$ in Ω along the iteration.

Here we use a variation of the reinitialization method in [31, section 7.4]. In other words, we solve the IVP $\phi_t - \tilde{\alpha} \Delta \phi - S_\beta(\varphi_k)(|\nabla \phi| - 1) = 0$, $t > 0$ with initial condition $\phi(0) = \varphi_k$. Here $S_\beta(\phi) := \text{sign}(\phi)$ for $|\phi| > \frac{\beta}{2}$, and zero elsewhere. The constant $\tilde{\alpha} > 0$ plays the role of a stabilization parameter: we use $\tilde{\alpha} = 0.01$ in crack scenario b_1^* and $\tilde{\alpha} = 0.005$ in crack scenarios b_2^* and b_3^* .

This reinitialization procedure of φ_k is implemented after every 10 iterations. No reinitialization is needed for the level-set function ψ_k .

5.3. Numerical results

The reconstruction results obtained for the three crack scenarios are presented in the figure 4. For each crack scenario b_k^* , $k = 1, 2, 3$, two levels of noise are considered, namely $\delta = 1\%$ and

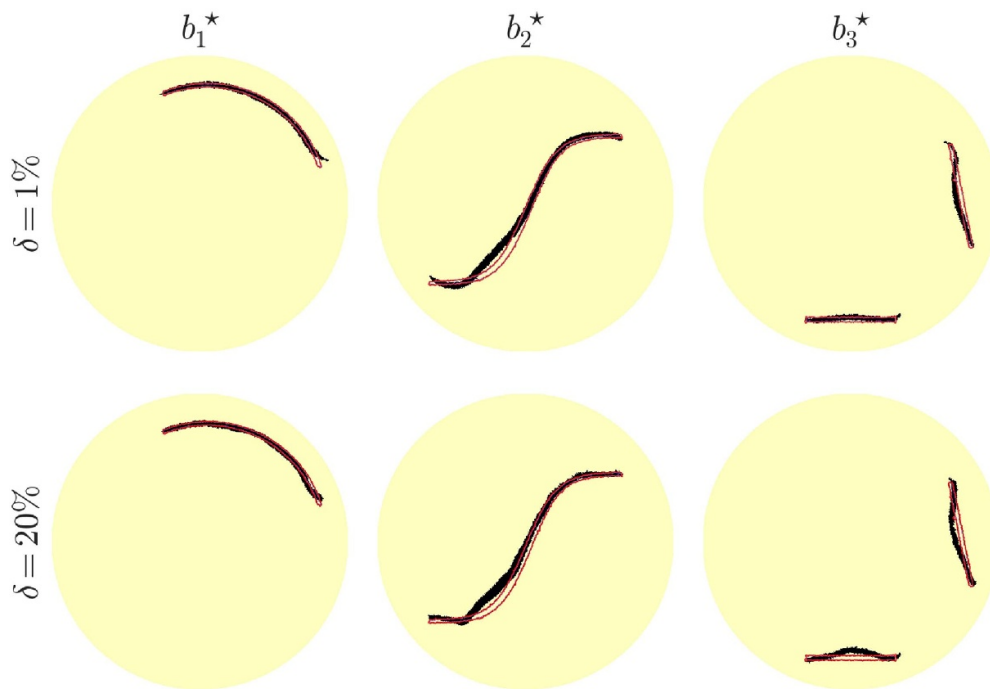


Figure 4. Reconstruction results. Crack scenarios are divided by columns. (FIRST ROW) noise level $\delta = 1\%$. (SECOND ROW) noise level $\delta = 20\%$.

$\delta = 20\%$. Each plot in this figure shows the contour of exact crack (RED) and the corresponding reconstruction (BLACK). The reconstructions are computed using $k = 1500$ iterations (for $\delta = 1\%$) and $k = 500$ (for $\delta = 20\%$).

In figure 5 the evolution of the *relative residual* and *relative iteration error* are presented in all three crack scenarios, and for both levels of noise.

Some considerations about the numerical experiments follow:

- Crack b_1^* is successfully reconstructed at both noise levels.
- The reconstruction quality of crack b_2^* deteriorates for the noise level $\delta = 20\%$. The curvature of b_2^* is recovered in both noise levels, but instabilities in the reconstruction appear as the noise level increases (a possible explanation is the fact that the Neumann data in section 5.1—using adjacent pattern—do not favor the reconstruction of information located in the interior of Ω ; see, e.g. [5]).
- The reconstruction of crack b_3^* represents the most challenging scenario. Since b_3^* consists of two disjoint cracks, we observe a geometry split in the evolution of level-set function ψ_k (see figure 7), which requires a large number of iterations. A detailed description of the evolution in this crack scenario is given at the end of this section (see figures 6 and 7).
- In all three crack scenarios the relative residual is monotonically decreasing; a few observed instabilities are related to the reinitialization procedure (see figure 5). On the other hand, the relative iteration error increases in the first iterations. A possible explanation is the fact that the zero level-sets of (φ_k, ψ_k) abruptly change in the first iterations (this is a well documented fact in the level-set literature; see, e.g. [17]).

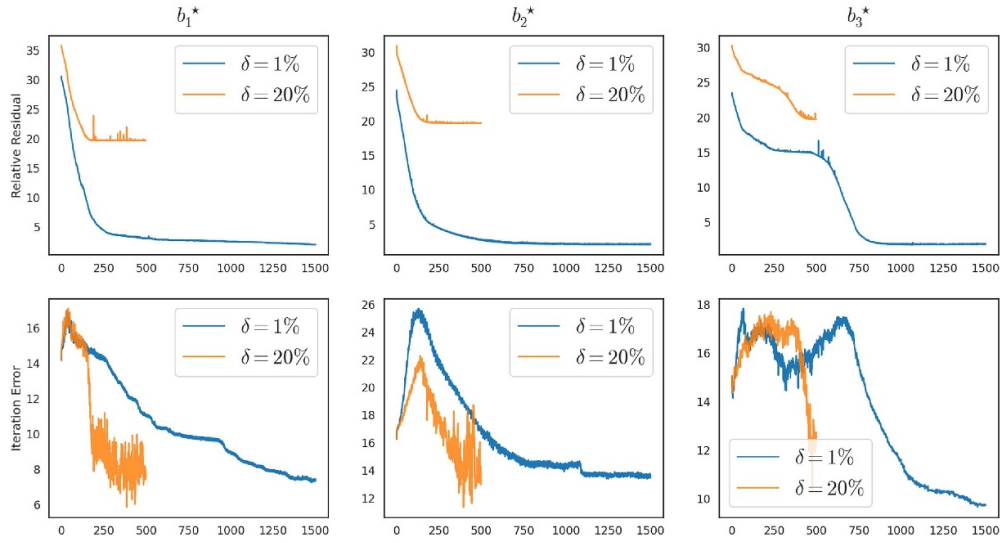


Figure 5. Evolution of relative residual (FIRST ROW) and relative iteration error (SECOND ROW). Crack scenarios are divided by columns.

- Iterative methods for ill-posed problems are commonly stopped according to the discrepancy principle [13]. Here the iterations are not stopped using discrepancy, since no theoretical results are available for our multiple level-set method. Instead, we observe the relative residual: the numerical experiments are terminated when the evolution of the relative residual stagnates (see first line in figure 5). Consequently, the experiments are terminated at either $k = 1500$ iterations (for $\delta = 1\%$) or $k = 500$ (for $\delta = 20\%$).

Next we present more details about the sequence (φ_k, ψ_k) produced by our method in crack scenario b_3^* with level of noise $\delta = 1\%$. In figure 6 the evolution of the reconstructed cracks $b_k = P_\varepsilon(\varphi_k, \psi_k)$ is presented. The initial guess consists of a single crack (see figure 3). At $k = 250$ steps the iteration b_k splits in two disconnected components. The evolution stagnates at $k = 1000$ steps (compare with figure 5, third column). In figure 7 the corresponding evolution of the level-set functions (φ_k, ψ_k) is presented (in all pictures of this figure, the zero level-sets of φ_k and ψ_k are plotted in black).

5.3.1. Revisiting the generation of Neumann/Dirichlet data

5.3.1.1. Choosing the number of NtD pairs. In all experiments above we used $N = 8$ pairs of Neumann/Dirichlet boundary data $\{(\eta_j, \gamma_j)\}_{j=1}^N$. It is worth mentioning that we also conducted numerical experiments for different values of N (ranging from 4 to 20) and observed that the use of a larger amount of NtD data may lead to a reconstruction of better quality (however, it certainly increases the numerical effort to run the iterative method).

In all crack scenarios b_i^* considered in this section, we observed that the choice $N = 8$ represents a fair balance between ‘accuracy of the reconstruction’ and ‘numerical effort’. In order to justify this assertion, we revisit in figure 8 the crack scenario b_2^* with noise level $\delta = 20\%$. The reconstruction results corresponding to the choices $N = 4, 8, 16$ are shown in this figure (the other parameters remain unchanged).

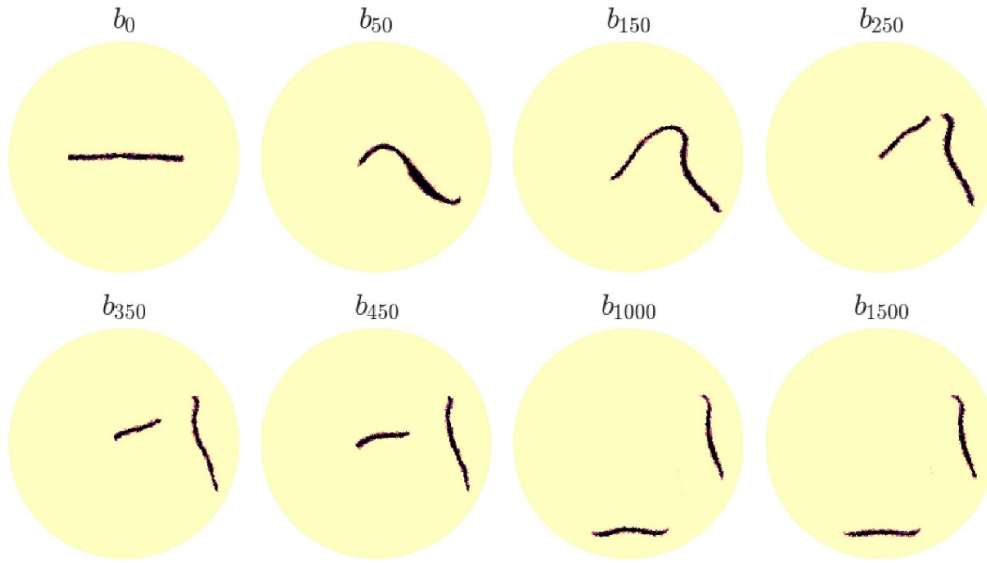


Figure 6. Crack scenario b_3^* with $\delta = 1\%$. Evolution of $b_k = P_\varepsilon(\varphi_k, \psi_k)$ for distinct values of k .

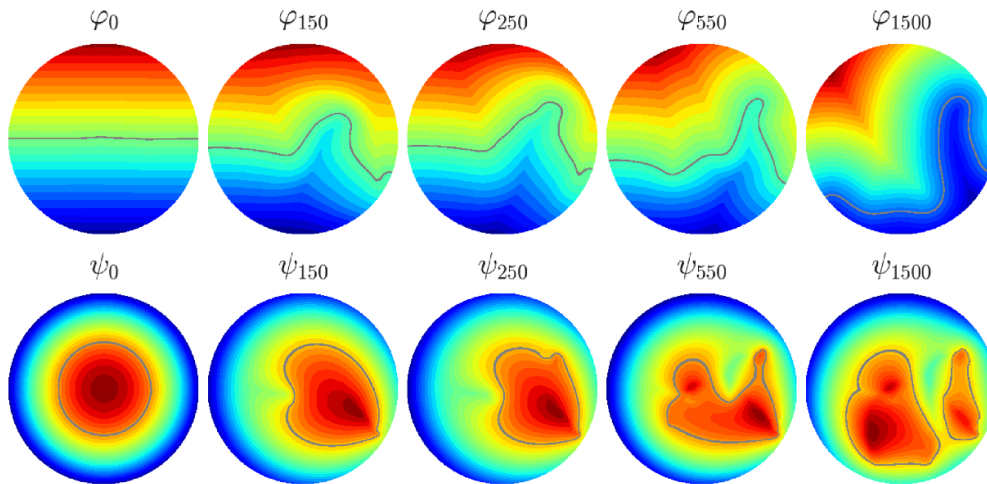


Figure 7. Crack scenario b_3^* with $\delta = 1\%$. Evolution of the level-set functions φ_k and ψ_k for distinct value of k .

5.3.1.2. The choice of the current pattern. In our experiments the adjacent current pattern $(1, -1, 0, 0, 0, 0, 0, 0)$ was used. We performed tests using other patterns, e.g. opposite pattern $(1, 0, 0, 0, -1, 0, 0, 0)$ and jump-one pattern $(1, 0, -1, 0, 0, 0, 0, 0)$. In all crack scenarios b_i^* we observed that the choice of current pattern do not strongly influence the quality of the reconstruction (crack scenario b_1^* with $\delta = 20\%$ is revisited in figure 9; reconstruction results using adjacent/opposite/jump-one current patterns are compared).

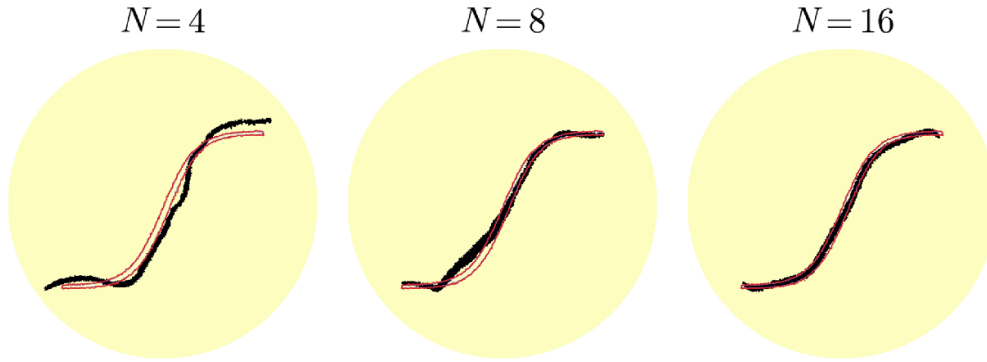


Figure 8. Crack scenario b_2^* revisited: $\delta = 20\%$ and adjacent current pattern. Reconstruction results for distinct values of N .

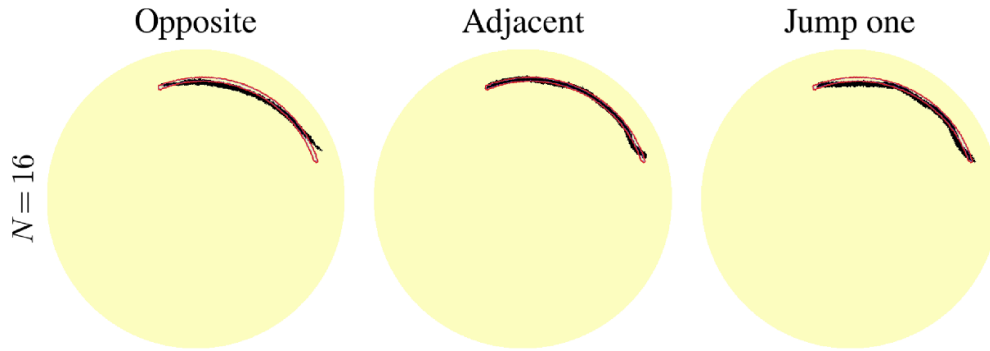


Figure 9. Crack scenario b_1^* revisited: $\delta = 20\%$ and $N = 16$. Reconstruction results for distinct current patterns.

5.3.1.3. The choice of the regularization parameters. Concerning the choice of parameters for the Tikhonov functional in (24), we follow [11, 17] in the numerical setup.

- μ_1, μ_2, μ_3 relate the BV-seminorm penalization and are small (or zero [17]);
- μ_4, μ_5 influence the stepsize for the updates $(\delta\varphi, \delta\psi)$ respectively, and usually $\mu_4 = \mu_5 = 1$ [11]. In crack scenario crack b_2^* , we chose a smaller value for μ_5 in order to stabilize the evolution of the level-set function ψ);
- we set $\varepsilon = \beta/4$ (the constant $\beta > 0$ is known); consequently, the thickness of the iterates $P_\varepsilon(\varphi_n, \psi_n)$ is compatible with the thickness of the exact solutions b_i^* .

6. Conclusions

In this article we introduce and analyze a hierarchical level-set approach for solving an inverse problem of crack identification in 2D-domains. The crack is modeled by two level-set functions: the first one represents the shape of the crack, while the second one determines the endpoints (by intersecting the first one). Based on this approach the Tikhonov functional \mathcal{G}_α using TV- H^1 penalization is introduced.

The concept of generalized minimizers in [10] is extended to the Tikhonov functional \mathcal{G}_α introduced here. Using this concept, coercivity and lower semi-continuity of the TV- H^1 penalization term is proven.

The first main contribution of this manuscript is the regularity result in proposition 4, where the L^1 -continuity of the parameter-to-output operator F (see (2)) is proven. This is necessary to prove the existence of minimizers of \mathcal{G}_α . Moreover, convergence and stability results are obtained. These results characterize our Tikhonov approach as a regularization method in the sense of [13, chapter 4].

For the purpose of numerical implementations, we introduce the smoothed functionals $\mathcal{G}_{\varepsilon,\alpha}$, and prove that the corresponding minimizers converge to a (generalized) minimizer of \mathcal{G}_α as $\varepsilon \rightarrow 0$.

The second main contribution of this manuscript consists in using the optimality conditions for $\mathcal{G}_{\varepsilon,\alpha}$ to derive a multiple level-set iterative method. In this context, our multiple level-set method can be interpreted as an iterated-Tikhonov type method for the smoothed functional $\mathcal{G}_{\varepsilon,\alpha}$ with small $\varepsilon > 0$.

Numerical experiments for the two-dimensional crack identification problem on a circular domain are used to verify the theoretical results using the iterative regularization algorithm presented in section 4.2 and detailed in algorithm 1. The numerical setting was built with synthetic Neumann/Dirichlet adjacent pattern data and artificially added noise. The level set iterations were performed with reinitialization steps in a constant fine mesh and the crack conductivity steps in an adaptive coarser mesh.

The numerical results show accurate reconstruction of simply/multiple connected cracks under the presence of noise. Moreover, these results are in agreement with the original purpose of the multiple level-set method proposed in these notes: while one of the level-set functions recover the shape of the crack, the other evolves to establish its endpoints.

Data availability statement

All data that support the findings of this study are included within the article (and any supplementary files).

Acknowledgments

A D C acknowledges support from CNPq, Grant 301499/2017-9 and from FAPERGS Grant PPP-ARD Grant 16/2551-0000211-8.

A L acknowledges support from CNPq, Grant 311087/2017-5, and from the Alexander von Humboldt foundation AvH.

E H acknowledges support from CNPq, Grant 163469/2021-0.

A O acknowledges ANID- Fondecyt 1191903, 1201311, CMM FB210005 Basal-ANID, FONDAPE/15110009, Millennium Program NCN19-161, ACIPDE MATH190008 and CYAN Cimat-Amsud project.

ORCID iDs

A De Cezaro  <https://orcid.org/0000-0001-8431-9120>

A Leitão  <https://orcid.org/0000-0001-6785-8835>

References

- [1] Adams R A 1975 *Sobolev Spaces* (New York: Academic)
- [2] Alnaes M S, Blechta J, Hake J, Johansson A, Kehlet B, Logg A, Richardson C, Ring J, Rognes M E and Wells G N 2015 The fenics project version 1.5 *Arch. Numer. Softw.* **3** 9–23
- [3] Álvarez D, Dorn O, Irishina N and Moscoso M 2009 Crack reconstruction using a level-set strategy *J. Comput. Phys.* **228** 5710–21
- [4] Ambrosio L 1989 Variational problems in SBV and image segmentation *Acta Appl. Math.* **17** 1–40
- [5] Borcea L 2002 Electrical impedance tomography *Inverse Problems* **18** R99
- [6] Boukari Y and Haddar H 2013 The factorization method applied to cracks with impedance boundary conditions *Inverse Problems Imaging* **7** 1123
- [7] Bruhl M, Hanke M and Pidcock M 2001 Crack detection using electrostatic measurements *ESAIM: Math. Modelling Numer. Anal.* **35** 595–605
- [8] Bryan K and Vogelius M S 2004 A review of selected works on crack identification *Geometric Methods in Inverse Problems and PDE Control (The IMA Volumes in Mathematics and its Applications vol 137)*, ed C B Croke, M S Vogelius, G Uhlmann and I Lasiecka (New York: Springer) pp 25–46
- [9] Charnley M and Vogelius M S 2020 A uniformly valid model for the limiting behaviour of voltage potentials in the presence of thin inhomogeneities I. The case of an open mid-curve *Asymptotic Anal.* **117** 215–40
- [10] De Cezaro A, Leitão A and Tai X-C 2009 On multiple level-set regularization methods for inverse problems *Inverse Problems* **25** 035004
- [11] De Cezaro A, Leitão A and Tai X-C 2013 On piecewise constant level-set (PCLS) methods for the identification of discontinuous parameters in ill-posed problems *Inverse Problems* **29** 015003
- [12] Dorn O and Lesselier D 2009 Level set methods for inverse scattering—some recent developments *Inverse Problems* **25** 125001
- [13] Engl H W, Hanke M and Neubauer A 1996 *Regularization of Inverse Problems (Mathematics and its Applications vol 375)* (Dordrecht: Kluwer Academic Publishers Group)
- [14] Evans L C 1998 *Partial Differential Equations (Graduate Studies in Mathematics vol 19)* (Providence, RI: American Mathematical Society)
- [15] Evans L C and Gariepy R F 1992 *Measure Theory and Fine Properties of Functions (Studies in Advanced Mathematics)* (Boca Raton, FL: CRC Press)
- [16] Friedman A and Vogelius M 1989 Determining cracks by boundary measurements *Indiana Univ. Math. J.* **38** 527–56
- [17] Frühauf F, Scherzer O and Leitão A 2005 Analysis of regularization methods for the solution of ill-posed problems involving discontinuous operators *SIAM J. Numer. Anal.* **43** 767–86
- [18] Gallouët T and Monier A 1999 On the regularity of solutions to elliptic equations *Rend. Mat. Appl.* **19** 471–88
- [19] Guo J and Zhu X 2021 The factorization method for cracks in electrical impedance tomography *Comput. Appl. Math.* **40** 20
- [20] Hallaji M and Pour-Ghaz M 2014 A new sensing skin for qualitative damage detection in concrete elements: rapid difference imaging with electrical resistance tomography *NDT&E Int.* **68** 13–21
- [21] Hallaji M, Seppänen A and Pour-Ghaz M 2014 Electrical impedance tomography-based sensing skin for quantitative imaging of damage in concrete *Smart Mater. Struct.* **23** 085001
- [22] Hauptmann A, Ikehata M, Itou H and Siltanen S 2018 Revealing cracks inside conductive bodies by electric surface measurements *Inverse Problems* **35** 025004
- [23] Hiles A J and Dorn O 2020 Sparsity and level set regularization for near-field electromagnetic imaging in 3D *Inverse Problems* **36** 025012
- [24] Hiles A J and Dorn O 2021 Colour level set regularization for the electromagnetic imaging of highly discontinuous parameters in 3D *Inverse Problems Sci. Eng.* **29** 489–524
- [25] Hou T-C, Loh K J and Lynch J P 2007 Spatial conductivity mapping of carbon nanotube composite thin films by electrical impedance tomography for sensing applications *Nanotechnology* **18** 315501
- [26] Ikehata M and Siltanen S 2000 Numerical method for finding the convex hull of an inclusion in conductivity from boundary measurements *Inverse Problems* **16** 1043–52
- [27] Isakov V 2006 *Inverse Problems for Partial Differential Equations (Applied Mathematical Sciences vol 127)* 2nd edn (New York: Springer)

- [28] Jauhainen J, Seppänen A and Valkonen T 2022 Mumford–Shah regularization in electrical impedance tomography with complete electrode model *Inverse Problems* **38** 065004
- [29] Kaptsov A V and Shifrin E I 2019 Identification of multiple cracks in an anisotropic elastic plate by boundary data *J. Phys.: Conf. Ser.* **1203** 012029
- [30] Meyers N G 1963 An L^p -estimate for the gradient of solutions of second order elliptic divergence equations *Ann. Scuola Norm. Sup. Pisa* **17** 189–206
- [31] Osher S and Fedkiw R 2003 *Level Set Methods and Dynamic Implicit Surfaces (Applied Mathematical Sciences)* (New York: Springer)
- [32] Shifrin E I and Kaptsov A V 2017 Identification of multiple cracks in 2D elasticity by means of the reciprocity principle and cluster analysis *Inverse Problems* **34** 015009
- [33] Smyl D and Liu D 2019 Invisibility and indistinguishability in structural damage tomography *Meas. Sci. Technol.* **31** 024001
- [34] Won-Kwang Park W-K 2017 Performance analysis of multi-frequency topological derivative for reconstructing perfectly conducting cracks *J. Comput. Phys.* **335** 865–84